



Short communication

# Platinum nanoparticles protected by a perfluorinated sulfonic acid copolymer: Preparation, nano-network formation and electrocatalytic activity

Hideo Naohara<sup>a</sup>, Takahiro Yoshimoto<sup>b</sup>, Naoki Toshima<sup>b,\*</sup><sup>a</sup> Toyota Motor Corporation, Susono, Shizuoka 410-0093, Japan<sup>b</sup> Tokyo University of Science Yamaguchi, Sanyo-Onoda, Yamaguchi 756-0884, Japan

## ARTICLE INFO

## Article history:

Received 9 June 2009

Received in revised form 31 August 2009

Accepted 1 September 2009

Available online 6 September 2009

## Keywords:

Nanoparticle

Electrocatalysis

Perfluorinated sulfonic acid copolymer

Fuel cells

Nano-network

## ABSTRACT

Platinum nanoparticles were successfully prepared in an aqueous solution using a perfluorinated sulfonic acid copolymer (PFSA) as a protecting agent. PFSA having good proton conductivity, gas permeability and chemical stability is used as a polyelectrolyte and an ionomer in catalyst layers of polymer electrolyte fuel cells. It was confirmed by infrared spectroscopy and in situ atomic force microscopy that the surface of nanoparticles was covered with PFSA molecules. In addition, PFSA-protected platinum nanoparticles formed the nano-network on dried films. Porous structures might improve the diffusion of reactants and products in the catalyst layer. The PFSA-protected platinum nanoparticles showed as good electrocatalytic activity for oxygen reduction reaction as a conventional Pt/C catalyst.

© 2009 Elsevier B.V. All rights reserved.

## 1. Introduction

It is well known that metal nanoparticles can be controlled in size, shape and dispersibility in a liquid phase by making use of water-soluble protecting agents such as poly(N-vinyl-2-pyrrolidone) (PVP) [1–5], surfactants [6–7], polyelectrolyte [8–11] and ionic liquid [12–13]. Protecting agents, however, sometimes deactivate catalytic reactions or inhibit the diffusion of reactants and products on the nanoparticle surface due to its strong interaction and insufficient gas permeability. So, additional procedures are required to remove the protecting agents before applying the nanoparticles to the electrocatalyst that shows the high activity and yield.

The perfluorinated sulfonic acid copolymers (PFSA), for example Nafion<sup>®</sup> (DuPont), Flemion<sup>®</sup> (Asahi Glass Co., Ltd.) or Aciplex<sup>®</sup> (Ashahi Kasei Chemicals Corp.), which have good proton conductivity, gas permeability and chemical stability, are commonly used not only for the electrolyte membrane but also for the catalyst layer as an ionomer in fuel cells. Full contact of the surface of all nanoparticles with the copolymer should enhance the proton conductivity and the platinum utilization ratio by making a good three-phase boundary for the electrochemical reaction. In this study, we achieved to use PFSA directly as the protecting agents for making metal nanoparticles in an aqueous solution. The cata-

lyst capped by the polymer electrolyte without the carbon support could exclude carbon corrosion and avoid the agglomeration of nanoparticles. In addition, we successfully tried to prepare PFSA-protected platinum nanoparticles with a nano-network structure to improve the gas diffusion, electric conductivity in a catalyst layer of actual fuel cells.

## 2. Experimental

Platinum nanoparticles protected by PFSA were prepared from hydrogen hexachloroplatinate(IV) hexahydrate (Wako Pure Chemical Industries) and Nafion<sup>®</sup> DE1020CS PFSA dispersion (DuPont Fuel Cells). A fixed volume of PFSA ( $R=5-0.005$ ) was mixed with Milli-Q water and hydrogen hexachloroplatinate(IV).  $R$  denotes a molar ratio of monomer unit of PFSA to platinum. After reduction of Pt ions by sodium tetrahydroborate (five times moles of  $H_2PtCl_6$  were used.), the produced Pt nanoparticles were purified and concentrated by ultrafiltration under argon at pressure of  $1.20-1.01\text{ kg cm}^{-2}$  with an ultrafilter (Advantec, Q0100 076E) and Milli-Q water several times until chloride ion was not detected in a filtrate solution. Finally, the dispersion of the PFSA-protected platinum (Pt/PFSA) nanoparticles was concentrated to 5–10 wt.% of metal content for the electrochemical measurements.

Electrochemical measurements were carried out by means of a rotating disk electrode (RDE). A conventional three-electrodes cell is equipped with a reversible hydrogen electrode (RHE) and platinum foil as a reference and counter electrodes, respectively. All the potentials in this paper are presented with respect to

\* Corresponding author. Tel.: +81 836 88 4561; fax: +81 836 88 4567.

E-mail address: [toshima@ed.yama.tus.ac.jp](mailto:toshima@ed.yama.tus.ac.jp) (N. Toshima).

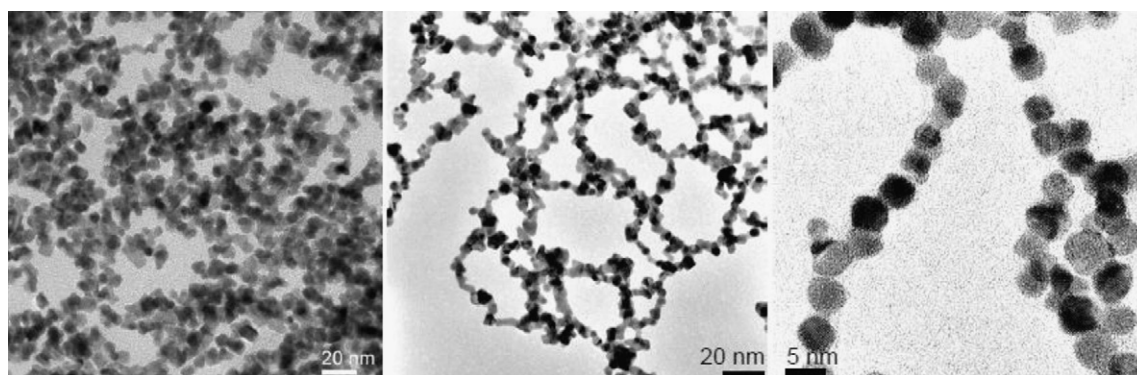


**Fig. 1.** TEM images of the Pt/PFSA nanoparticles prepared at  $R=0.005$  (a) before and (b) after the purification and concentration procedure. Pt/PFSA colloidal solutions were concentrated to 1/40. (c) Magnified TEM image of Pt/PFSA nanoparticles.

the RHE. The sample electrode was prepared by direct drop of  $20 \mu\text{g platinum cm}^{-2}$  of the Pt/PFSA nanoparticles onto a rotating electrode surface made of grassy carbon then dried under a nitrogen flow. Platinum content in the colloidal solution was analyzed by an inductively coupled plasma atomic emission spectrometry (ICP-AES). Commercially available Ketjen black supported 50 wt.% platinum catalyst (Pt/C) was used as a reference catalyst. Electrochemical measurements were carried out in an argon or oxygen saturated  $0.1 \text{ mol l}^{-1}$  perchloric acid solution.

### 3. Results and discussion

Reduction of metal ion in the solution was confirmed by ultraviolet and visible spectroscopy (UV-vis) before and after the reduction. A large absorption peak and a small shoulder, assigned to d-d transition and ligand-to-metal charge-transfer transition of  $[\text{PtCl}_6]^{2-}$ , were observed at 260 nm and 380 nm before the reduction [14]. After 1 h refluxing, the absorption peaks at 260 nm and 380 nm disappeared completely and a broad tailing absorption was observed. This indicates that  $[\text{PtCl}_6]^{2-}$  was reduced to platinum metal completely even under existing of PFSA. The dark dispersion of the Pt/PFSA nanoparticles is quite stable against aggregation over several months.

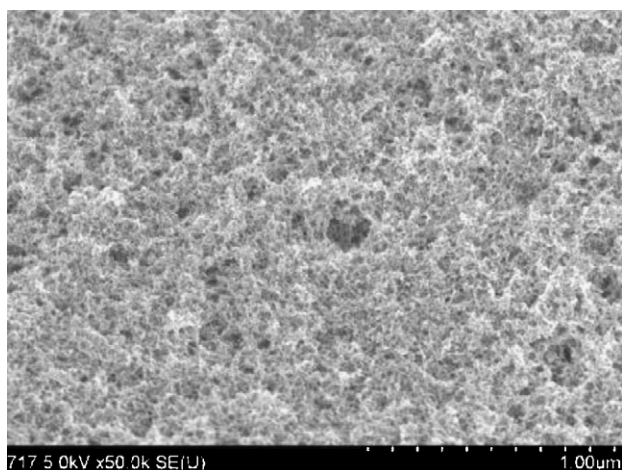
The structures and mean diameter of the Pt/PFSA nanoparticles ( $R=5, 1, 0.5$  and  $0.005$ ) were characterized by high-resolution transmission electron microscopy (HR-TEM). Fig. 1 shows TEM images of the Pt/PFSA nanoparticles at  $R=0.005$  (a) before and (b) after the purification and concentration procedure. The Pt/PFSA colloidal solutions were finally concentrated to 1/40. Before the purification and concentration, The Pt/PFSA nanoparticles were formed homogeneously into average diameter of ca. 5 nm. After those procedures, the Pt/PFSA nanoparticles consisting of the primary particles of average diameter of ca. 5 nm were lined forming nano-wires and a nano-network. Particle sizes were almost the same in each  $R$  ratios, and specific shapes such as cubic, tetrahedron or cuboctahedron were not observed. The nano-network was observed clearly after the purifying and concentration, and a mesh size of the nano-network was not dependent on the concentration ratio of the Pt/PFSA nanoparticles. Lining of nanoparticles was investigated by the lattice analysis from HR-TEM images (Fig. 1c). In the case of citrate-protected gold nanoparticles that formed nano-wires, Xie et al. reported that the lattices of each gold nanoparticles lined in same direction and nanoparticles connected at the specific crystalline faces each other [15]. In the case of the Pt/PFSA nanoparticles, each platinum nanoparticles showed different lattice directions and were not connected at the specific faces each other, that is, platinum nano-wire growth was not depended on the direction of the crystal lattice.

Usually metal nanoparticles are well dispersed in water and/or alcohol by protection of water-soluble polymers like PVP, where the coordination of carbonyl group of PVP to metal nanoparticle surface has been proved by infrared (IR) spectroscopy [16]. Thus, the interaction between platinum nanoparticles and PFSA molecules was investigated by IR spectroscopy. Besides the absorption peaks at 530 (C-F bending, S-O bending), 636 (C-F bending), 970–980 (C-O-C symmetric stretching), 1050 (symmetric  $-\text{SO}_3^-$  stretching), 1149 (symmetric C-F stretching of backbone) and 1234 (asymmetric C-F stretching of backbone)  $\text{cm}^{-1}$  observed in PFSA without nanoparticles [17,18], we observed additional absorption peaks at 1150–1250 (symmetric and asymmetric C-F stretching)  $\text{cm}^{-1}$  for Pt/PFSA nanoparticles at  $R=0.05$  (Figure S1). Furthermore, the broad absorption peak around 1410 (S=O stretch of  $-\text{SO}_3\text{H}$ )  $\text{cm}^{-1}$  was observed at  $R=0.005$ . We cannot distinguish clearly the peak at  $1120 \text{ cm}^{-1}$  assigned to  $-\text{SO}_3^-$  group adsorbed on platinum surface [17] because of the large absorption peak of C-F stretching around  $1150 \text{ cm}^{-1}$ . But increasing the absorption of the broad peak around  $1410 \text{ cm}^{-1}$  at  $R=0.005$  means it reflects mainly the information of the interface, i.e., protonated  $-\text{SO}_3\text{H}$  groups adsorb on the platinum nanoparticle surface [18]. So, it could be concluded that PFSA coordinates to the platinum surface and should play as protecting agents even in the nanoparticle dispersion.

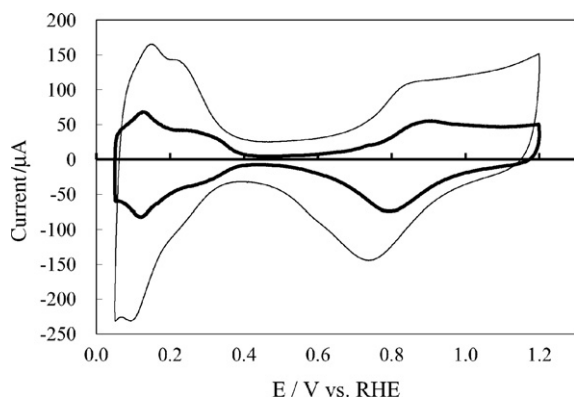
We also observed directly the Pt/PFSA nanoparticles ( $R=0.005$ ) dried on a highly oriented pyrolytic graphite (HOPG) substrate after ultrafiltration by means of in situ tapping mode atomic force microscopy (AFM). Bright spots were observed on the substrate surface in ambient conditions (Figure S2a). The surface images observed by AFM are similar to those observed by TEM, but the observed spots were quite different from the images of the aggregates of PFSA without Pt nanoparticles [19]. Thus, we concluded that observed particles were dried Pt/PFSA nanoparticles. After observing a topograph of dried nanoparticles, Milli-Q water was dropped onto the dried nanoparticles. Diameter of bright spots was changed to larger (Figure S2b). This should be due to swelling of PFSA on the surface of Pt nanoparticles. The results from IR and AFM support the fact that PFSA exists on the surface of the platinum nanoparticles even after ultrafiltration and plays a role not only as an ionomer but also as a protecting agent.

Fig. 2 shows a scanning electron microscopy (SEM) image of the Pt/PFSA nanoparticles dropped on a flat silicon substrate followed by dried at room temperature under ambient pressure. The Pt/PFSA nanoparticles stacked, however, construct a porous catalyst layer with keeping the nano-network structure. We conclude that the Pt/PFSA nanoparticles with the nano-network can form the porous catalyst layer and it should be effective for diffusion of reactants and products in the electrode assembly.

Fig. 3 shows CVs of the Pt/PFSA nanoparticles ( $R=0.005$ ) and a conventional platinum catalyst supported on carbon (Pt/C) in argon



**Fig. 2.** SEM image of the Pt/PFSA nanoparticles dropped on a flat silicon substrate followed by dried at room temperature under ambient pressure.



**Fig. 3.** Cyclic voltammograms of the Pt/PFSA nanoparticles ( $R=0.005$ ) and a carbon supported-platinum catalyst (Pt/C) in an argon saturated  $0.1 \text{ mol l}^{-1}$  perchloric acid solution. Sweep rate =  $50 \text{ mV s}^{-1}$ .

saturated  $0.1 \text{ mol l}^{-1}$  perchloric acid solution. Typical CV profile of platinum was observed at the Pt/PFSA nanoparticles. Electrochemical surface area (ECSA) of platinum nanoparticles calculated by the charge of hydrogen desorption was  $32.1 \text{ m}^2 \text{ g}^{-1}\text{-Pt}$ . This value is larger than that of platinum black ( $15\text{--}20 \text{ m}^2 \text{ g}^{-1}\text{-Pt}$ ), but much smaller than that of the Pt/C ( $70.8 \text{ m}^2 \text{ g}^{-1}\text{-Pt}$ ) due to the difference in the platinum particle size and dispersion. ECSA was, however, decreased obviously at  $R > 1$ . Some Pt/PFSA nanoparticles seem to be isolated in the catalyst layer due to the excess of the protecting ionomer even if the formation of the nano-network improves the electric conductivity.

Fig. 4 shows anodic linear sweep voltammograms of the Pt/PFSA nanoparticles ( $R=0.005$ ) and Pt/C in an oxygen saturated  $0.1 \text{ mol l}^{-1}$  perchloric acid solution at 900 rpm. Each oxygen reduction currents were subtracted blank currents recorded in the argon saturated solution, respectively. A half wave potential of oxygen reduction of the Pt/PFSA nanoparticles shifts to 906 mV by 8 mV from the value of Pt/C. Kinetic currents of the Pt/PFSA nanoparticles and Pt/C analyzed by Koutecký–Levich plot [20] were 198 and  $174 \text{ mA mg-Pt}^{-1}$  at 0.9 V, respectively. We have confirmed that the Pt/PFSA nanoparticles realized good electrocatalytic mass-activity for oxygen reduction reaction at the same level as the conventional Pt/C catalyst. As the stable metal colloid solution with the nano-network is easy to assemble the catalyst layer by the existing coating equipments without any dispersing procedures

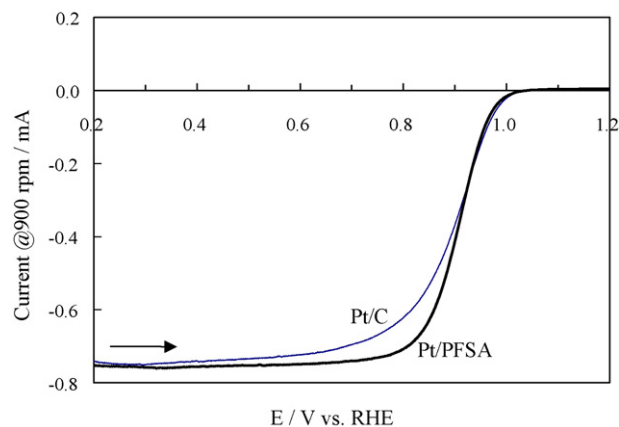


**Fig. 4.** Linear sweep voltammograms of the Pt/PFSA nanoparticles ( $R=0.005$ ) and Pt/C in an oxygen saturated  $0.1 \text{ mol l}^{-1}$  perchloric acid solution at 900 rpm. Each oxygen reduction currents were subtracted blank currents recorded in the argon saturated solution, respectively. Sweep rate =  $20 \text{ mV s}^{-1}$ .

of the catalyst ink, it is very useful for the Pt/PFSA nanoparticles to apply to actual fuel cell electrodes with the low cost. A MEA evaluation of the Pt/PFSA nanoparticles is under investigation.

#### 4. Conclusion

Platinum nanoparticles of ca. 5 nm diameter were successfully prepared in an aqueous solution using PFSA as a protecting agent. In addition, the Pt/PFSA nanoparticles formed the nano-network on dried films. The Pt/PFSA nanoparticles realized good electrocatalytic mass-activity for oxygen reduction reaction at the same level as the conventional Pt/C catalyst.

#### Appendix A. Supplementary data

Supplementary data associated with this article can be found, in the online version, at doi:10.1016/j.jpowsour.2009.09.002.

#### References

- [1] N. Toshima, T. Yonezawa, *New J. Chem.* 22 (1998) 1179.
- [2] A. Wieckowski, E.R. Savinova, C.G. Vayenas (Eds.), *Catalysis and Electrocatalysis at Nanoparticle Surfaces*, Marcel Dekker, New York, 2003, p. 379, Chapter 11.
- [3] B. Corain, G. Schmid, N. Toshima (Eds.), *Metal Nanoclusters in Catalysis and Materials Science: The Issue of Size Control*, Elsevier, Amsterdam, 2008.
- [4] R. Narayanan, M.A. El-Sayed, *Top. Catal.* 47 (2008) 15.
- [5] M.M. Koebel, L.C. Jones, G.A. Somorjai, *J. Nanoparticle Res.* 10 (2008) 1063.
- [6] C. Wang, H. Daimon, T. Onodera, T. Koda, S.H. Sun, *Angew. Chem. Int. Ed.* 47 (2008) 3588.
- [7] F.R. Fan, D.Y. Liu, Y.F. Wu, S. Duan, Z.X. Xie, Z.Y. Jiang, Z.Q. Tian, *J. Am. Chem. Soc.* 130 (2008) 6949.
- [8] R.L. McCreery, *Chem. Rev.* 108 (2008) 845.
- [9] Z.Q. Tian, S.P. Jjiang, Z. Liu, L. Li, *Electrochem. Commun.* 9 (2007) 1613.
- [10] G. Schmid (Ed.), *Nanoparticles*, WILEY-VCH, Weinheim, 2008.
- [11] J. Koetz, S. Kosmella, *Polyelectrolytes and Nanoparticles*, Springer, New York, 2007.
- [12] V.I. Parvulescu, C. Hardacre, *Chem. Rev.* 107 (2007) 2615.
- [13] F. Endres, A.P. Abbott, D.R. MacFarlane (Eds.), *Electrodeposition from Ionic Liquids*, WILEY-VCH, Weinheim, 2008.
- [14] A. Henglein, B.G. Ershov, M. Malow, *J. Phys. Chem.* 99 (1995) 14129.
- [15] J. Xie, Q. Zhang, J.Y. Lee, D.I.C. Wang, *J. Phys. Chem. C* 111 (2007) 17158.
- [16] H. Hirai, H. Chawanya, N. Toshima, *React. Polym.* 3 (1985) 127.
- [17] Y. Ayato, K. Kunimatsu, M. Osawa, T. Okada, *J. Electrochem. Soc.* 153 (2006) A203.
- [18] D. Malevich, V. Zamylny, S.-G. Sun, J. Lipkowski, *Z. Phys. Chem.* 217 (2003) 51.
- [19] T. Masuda, H. Naohara, S. Takakusagi, P.R. Singh, K. Uosaki, *Chem. Lett.* 38 (2009) 884.
- [20] U.A. Paulus, T.J. Schmidt, H.A. Gasteiger, R.J. Behm, *J. Electroanal. Chem.* 295 (2001) 134.